

UC Berkeley

UC Berkeley Previously Published Works

Title

An overview of the Daya Bay reactor neutrino experiment

Permalink

<https://escholarship.org/uc/item/0gp7n2rj>

Authors

Cao, Jun

Luk, Kam-Biu

Publication Date

2016-07-01

DOI

10.1016/j.nuclphysb.2016.04.034

Peer reviewed



An overview of the Daya Bay reactor neutrino experiment

Jun Cao ^a, Kam-Biu Luk ^b

^a *Institute of High Energy Physics, Beijing, China*

^b *Department of Physics, University of California and Lawrence Berkeley National Laboratory, Berkeley, CA, USA*

Received 18 February 2016; received in revised form 21 April 2016; accepted 21 April 2016

Available online 26 April 2016

Editor: Tommy Ohlsson

Abstract

The Daya Bay Reactor Neutrino Experiment discovered an unexpectedly large neutrino oscillation related to the mixing angle θ_{13} in 2012. This finding paved the way to the next generation of neutrino oscillation experiments. In this article, we review the history, featured design, and scientific results of Daya Bay. Prospects of the experiment are also described.

© 2016 The Authors. Published by Elsevier B.V. This is an open access article under the CC BY license (<http://creativecommons.org/licenses/by/4.0/>). Funded by SCOAP³.

1. Introduction

Neutrino oscillation was firmly established by 2002. Around that time, atmospheric and accelerator neutrino experiments, e.g. Super-K [1] and K2K [2], have determined the oscillation parameters θ_{23} and $|\Delta m_{32}^2|$ whereas solar and reactor neutrino experiments, such as SNO [3] and KamLAND [4], have measured θ_{12} and Δm_{21}^2 . However, the mixing angle θ_{13} , the CP violating phase δ_{CP} , and the sign of Δm_{32}^2 (aka the mass hierarchy) were unknown. In addition, θ_{13} , unlike the other two mixing angles, was expected to be small [5,6].

Among the three unknown quantities, θ_{13} plays a critical role in defining the future experimental program on neutrino oscillation. It is known that the CP-violating effect is proportional

E-mail addresses: caoj@ihep.ac.cn (J. Cao), k_luk@berkeley.edu (K.B. Luk).

to

$$J = \sin 2\theta_{12} \sin 2\theta_{23} \sin 2\theta_{13} \cos \theta_{13} \sin \delta_{\text{CP}} \approx 0.9 \sin 2\theta_{13} \sin \delta_{\text{CP}}. \quad (1)$$

Resolution of the mass hierarchy problem also relies on the size of θ_{13} . If it is too small, current technologies may not be able to determine δ_{CP} and the mass hierarchy.

The mixing angle θ_{13} can be measured by accelerator-based or reactor-based experiments. However, the appearance probability of $\nu_{\mu} \rightarrow \nu_e$ in an accelerator neutrino experiment also depends on the yet unknown δ_{CP} and the mass hierarchy. Hence, this type of experiments can only provide evidence for a non-zero θ_{13} but cannot measure its value unambiguously at this moment. On the other hand, reactor-based experiments can unambiguously determine θ_{13} via measuring the survival probability of the electron antineutrino $\bar{\nu}_e$ at short distance ($\mathcal{O}(\text{km})$) from the reactors. In the three-neutrino framework, the survival probability is given by

$$P = 1 - \cos^4 \theta_{13} \sin^2 2\theta_{12} \sin^2 \Delta_{21} - \sin^2 2\theta_{13} \sin^2 \Delta_{ee}, \quad (2)$$

where $\sin^2 \Delta_{ee} \equiv \cos^2 \theta_{12} \sin^2 \Delta_{31} + \sin^2 \theta_{12} \sin^2 \Delta_{32}$ and $\Delta_{ji} \equiv 1.267 \Delta m_{ji}^2 L/E$ with Δm_{ji}^2 being the mass-squared difference in eV^2 , E is the energy of the $\bar{\nu}_e$ in MeV, and L is the distance in meters from the production point.

Pinning down θ_{13} by performing a relative measurement with a set of near and far detectors was suggested at the beginning of this millennium [7]. This method allows cancellation of most of the systematic uncertainties due to the reactor and the detector that previous experiments suffered. Since 2002, eight reactor experiments were proposed [8]; three of them, Daya Bay [9], Double Chooz [10], and RENO [11], were constructed.

Among the eight proposals, the Daya Bay experiment is the most sensitive for measuring θ_{13} . The nuclear-power complex is among the top five most powerful in the world, providing a very intense flux of antineutrinos. In addition, it is very close to a mountain range in which an array of horizontal tunnels can be built, providing sufficient overburden to attenuate cosmic rays and space to accommodate a relatively large-scale experiment.

The Daya Bay nuclear-power complex is located on the southern coast of China, 55 km to the northeast of Hong Kong and 45 km to the east of Shenzhen. As shown in Fig. 1, the nuclear complex consists of six reactors grouped into three pairs, with each pair referred to as a nuclear power plant (NPP). All six cores are functionally identical pressurized water reactors, each with a maximum of 2.9 GW of thermal power. The last core started commercial operation on 7 August 2011, a week before the start-up of the Daya Bay experiment. The distance between the cores for each pair is 88 m. The Daya Bay cores are separated from the Ling Ao cores by about 1100 m, while the Ling Ao-II cores are around 500 m away from the Ling Ao cores.

The Daya Bay experiment consists of three underground experimental halls (EHs) connected with horizontal tunnels. The overburden for the Daya Bay near hall (EH1), the Ling Ao near hall (EH2) and the far hall (EH3) are 250, 265, and 860 equivalent meters of water, respectively. Eight antineutrino detectors (ADs) are installed in the three halls, with two in EH1, two in EH2, and four in EH3. Each AD has 20-ton target mass to catch the reactor antineutrinos. The sensitivity to $\sin^2 2\theta_{13}$ was designed to be better than 0.01 at 90% confidence level in 3 years.

2. History of the Daya Bay experiment

The idea of determining θ_{13} using the Daya Bay reactor complex was proposed in 2003. The first dedicated workshop for the Daya Bay experiment was held in the University of Hong Kong in November 2003 [12]. It was immediately followed by the second one in January 2004

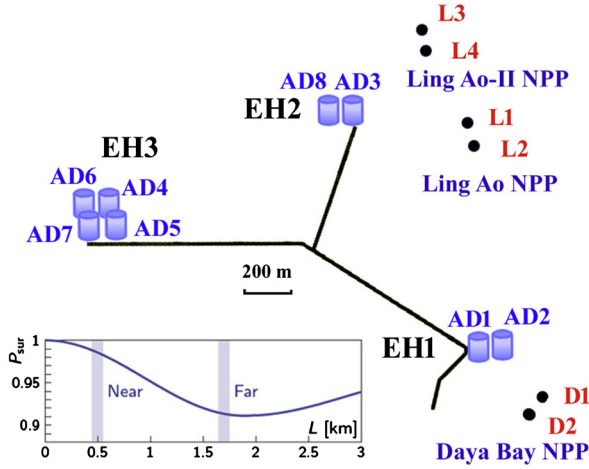


Fig. 1. Layout of the Daya Bay experiment. The dots represent the reactor cores, labeled as D1, D2, L1 to L4. Eight antineutrino detectors, labeled as AD1 to AD8, are installed in three underground experimental halls (EH1–EH3). The bottom sub-panel shows the survival probability as a function of the effective baseline L . The near and far detectors locate in the shaded area.

at the Institute of High Energy Physics [13], at which a preliminary experimental design was presented, including the unique multiple-detector scheme and the reflective panel design for light collection. In response to the recommendation of measuring $\sin^2 2\theta_{13}$ to the level of 0.01 by the APS Neutrino Study [14] and NuSAG [15], the target mass of the detectors was enlarged from 8 ton to 20 ton. The Conceptual Design Report (CDR) was released at the end of 2006 [9].

The Daya Bay Collaboration was officially formed in February 2006. The project was approved by the Chinese Academy of Sciences in May 2006 and by the Ministry of Science and Technology of China in January 2007. It passed the CD-2 review as required by the US Department of Energy in January 2008.

Ground breaking of the experiment took place in October 2007. Detectors were assembled onsite in parallel to the civil construction. After 4 years of construction, the first of the three underground experimental halls, EH1, started data taking on August 11, 2011. Data was used to study the detector performance, resulting a paper submitted on 28 February 2012 [16]. This publication reported that the relative detection uncertainty of two ADs was only 0.2%, much better than the designed value of 0.38% documented in the CDR.

Since the detector fabrication was out of sync with the civil construction, the collaboration decided to operate the experiment with two phases to maximize the scientific reach. The first phase was run with 6 ADs out of a total of 8, with two in EH1, one in EH2, and three in EH3. The second near hall, EH2, was ready on 5 November 2011, and EH3 started data taking on 24 December 2011. On 8 March 2012, the Daya Bay Collaboration announced the discovery of a new disappearance of reactor antineutrinos at 5.2 standard deviations (σ) and measured $\sin^2 2\theta_{13} = 0.092 \pm 0.016(\text{stat}) \pm 0.005(\text{syst})$ with 55 days data [17]. It was further verified at 7.7σ with 139 days of data [18], and at 4.6σ with a statistically independent data set using antineutrino events tagged by neutron capture on hydrogen [19].

The six-detector phase terminated on 28 July 2012. The last two ADs were installed. The full configuration of the Daya Bay experiment started data taking on 19 October 2012, running reliably to present. Two additional results on neutrino oscillation were reported subsequently.

Table 1

Daya Bay measurements on $\sin^2 2\theta_{13}$ and Δm_{ee}^2 . The first uncertainty of $\sin^2 2\theta_{13}$ in the first two rows is the statistical error and the second is the systematic one. The unit of Δm_{ee}^2 is 10^{-3} eV^2 .

Release time	Data	Config	$\sin^2 2\theta_{13}$	Δm_{ee}^2
2012/3/8 [17]	55 days	6 ADs	$0.092 \pm 0.016 \pm 0.005$	–
2012/10/23 [18]	139 days	6 ADs	$0.089 \pm 0.010 \pm 0.005$	–
2013/10/24 [20]	217 days	6 ADs	$0.090_{-0.009}^{+0.008}$	$2.59_{-0.20}^{+0.19}$
2014/6/24 [19]	217 days	6 ADs (nH)	0.083 ± 0.018	–
2015/5/13 [21]	621 days	6 + 8 ADs	0.084 ± 0.005	2.42 ± 0.11

With all 217 days of data acquired in the first phase, a spectral and rate analysis improved the precision of θ_{13} and measured the effective mass splitting Δm_{ee}^2 for the first time [20]. A new analysis with 621 days of data, including the 6-AD phase and the full 8-AD configuration, was released recently; the measured $\sin^2 2\theta_{13}$ has reached a precision of 6% [21]. These results are summarized in Table 1.

Daya Bay has accumulated the largest reactor antineutrino sample in the world, which enables many precision measurements. The most precise reactor antineutrino spectrum has been measured [22]. A search for a sterile neutrino has significantly extended the exclusion area in the low-mass region of the $\sin^2 2\theta_{14} - \Delta m_{41}^2$ parameter space [23]. Many exotic searches are ongoing. The Daya Bay experiment plans to operate until 2020. A 3%-precision measurement on both $\sin^2 2\theta_{13}$ and Δm_{ee}^2 is expected.

3. Design and features

In a reactor neutrino experiment, the sensitivity or precision in θ_{13} depends on how well the rate deficit and distortion in the energy spectrum are determined. When the exposure, defined as the product of the target mass of the far site detector in tons, the thermal power of the reactor in GW, and the live time in years, is larger than 10,000 GW-ton-yr, distortion in the energy spectrum, thus statistics, will dominate the sensitivity [24]. Such exposure corresponds to about 8 years for Daya Bay. Therefore, for most cases, the rate deficit will dominate the sensitivity, and related systematic uncertainties, including the detection efficiency, target proton number, and backgrounds, should be controlled to $\lesssim 0.5\%$ to measure $\sin^2 2\theta_{13}$ to 0.01 at 90% confidence level.

When multiple reactor cores are spread out over a large area, a single near site can only constrain the antineutrino flux from the nearby cores. In this case, the reactor-related uncertainties cannot be completely canceled by the near-far relative measurement. Moving the near site farther away from the cores will improve the cancellation but lose sensitivity due to an increase in the oscillation effect. To obtain the best sensitivity, Daya Bay is configured with one far site for observing the maximal oscillation effect, and two near sites for determining the flux of the reactor antineutrinos from the Daya Bay and Ling Ao NPPs. The best locations of the three halls were determined with a χ^2 method [25], with the projected uncertainties and estimated background at the candidate sites derived from the surveyed geological information. For the optimal configuration, the uncertainty related to the reactors is reduced to 5% of the uncorrelated uncertainty of a single core (0.8%), which is totally insignificant.

Experience and lessons learned in CHOOZ [5], Palo Verde [6], and KamLAND [4] were taken into account in designing the Daya Bay detectors. Some unique features of the Daya Bay design significantly improve the detector performance; indeed, the built-in redundancy is crucial for precision measurements. Details of the Daya Bay detector design and fabrication can be found in Ref. [26]. In the following we will briefly describe the experimental design highlighting the con-

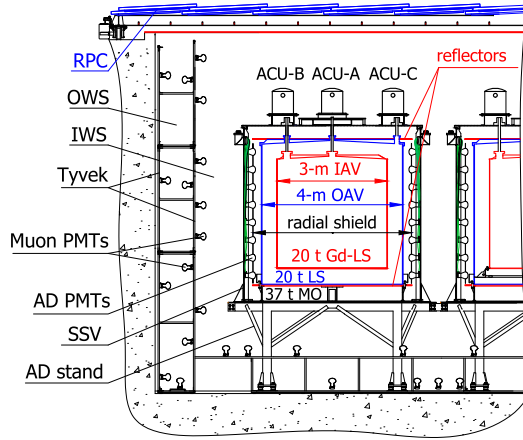


Fig. 2. Schematic diagram of the Daya Bay detectors.

cept of multiple muon taggers, multiple antineutrino detectors, a remote-controlled calibration system, photon reflectors and shields, as well as the optimization of the detector dimensions.

Each AD has three nested cylindrical volumes separated by concentric acrylic vessels as shown in Fig. 2. Serving as the target for the inverse beta-decay reaction, the innermost volume holds 20 t of gadolinium-doped liquid scintillator (Gd-LS) with 0.1% Gd by weight [27–30]. The middle volume is called the gamma catcher and is filled with 20 t of undoped liquid scintillator (LS) for detecting gamma-rays that escape the target volume. The outer volume contains 37 t of mineral oil (MO) to provide optical homogeneity and to shield the inner volumes against radiation from the detector components. There are 192 20-cm PMTs (Hamamatsu R5912) installed in the MO volume and around the circumference of the stainless steel vessel (SSV). The top and the bottom surfaces are not instrumented with PMTs; instead, there are two highly reflective panels. The PMTs are recessed in a 3-mm-thick black cylindrical shield located at the equator of the PMT bulb. In each hall, the ADs are submerged in a water pool that provides at least 2.5 m of water to degrade radiation from the rock. The water pool is optically divided into the inner (IWS) and outer (OWS) regions, both equipped with 20-cm PMTs to serve as water Cherenkov detectors. On the top of the water pool, there are Resistive Plate Chambers (RPCs) serving as another muon detector.

The multiple-module scheme is the most prominent feature of Daya Bay. The current generation of reactor neutrino experiments for determining θ_{13} planned to achieve a relative detector uncertainty of (0.38–0.6)%. Such level of uncertainties needs very careful validation. With at least two ADs in each experimental hall, comparison of performance among the ADs at the same site can actually “measure” the relative uncertainty between them. By comparing the components of the detector response, the relative uncertainty of the two ADs was found to be 0.2% [16]. The measured ratio of the antineutrino rates in the two ADs was 0.981 ± 0.004 (1.019 ± 0.004) while the expected ratio was 0.982 (1.012) for the Daya Bay (Ling Ao) near site [21], validating the estimation of relative uncertainty. The deviation from unity is due to slightly different baselines of the two ADs to the reactor cores. Furthermore, the uncertainties of the ADs are found to be largely uncorrelated. Therefore, the total relative detector uncertainty is statistically reduced by $1/\sqrt{N}$, where N is the number of ADs at a given site.

The water pool is divided into two water Cherenkov detectors, as shown in Fig. 2. The outer one is 1-m thick and the inner one is 1.5 m. The top of the water pool is covered by RPC tiles. The

outer Cherenkov counter and the RPC play important roles in determining the fast-neutron background originating from muon-induced spallation in the surrounding rock. The efficiency of the water Cherenkov detectors for detecting muons was designed to be 95%, and 90% for the RPCs. The combined efficiency was aimed to be $(99.5 \pm 0.25)\%$. As it turned out, due to high reflectivity of the custom-made Tyvek[®] composite film lining the partitions and the well-designed water purification system, the efficiency of the inner Cherenkov detector was 99.98% [32]. Again, the multiple-detector design provides robust tagging of the cosmic-ray muons, which is essential for rejecting muon-induced background.

The geometry of the AD was optimized with extensive Monte Carlo simulation. The MO shielding is thin, and the distance from the apex of the PMT to the liquid scintillator is only 20 cm. This distance is driven by the requirement of uniform detector response instead of radiation shielding. As a result, Daya Bay has a relatively high singles rate and accidental coincidence but maximized target mass. Since the accidental-coincidence background can be determined accurately to high precision, it has negligible impact to the sensitivity or precision.

To obtain good light yield with fewer number of PMTs, reflective panels are used. A specular reflective film with reflectivity $> 98\%$ in the scintillation light region, ESR (3M[®]), is sandwiched between two 1-cm-thick acrylic panels 4.5 m in diameter. The space between the two acrylic panels is evacuated when the panels are bonded together along the edge. As a result, a laminated reflector is formed with minimal mechanical connections between the two panels while achieving the optimal optical performance. A reflector is put on the top of the gamma catcher and another at the bottom. Such a design reduces the number of PMTs by about one half while achieving almost the same energy and vertex resolutions. Furthermore, the mechanical structure of the AD is simplified with the adoption of reflective panels, enabling transportable ADs.

Three water-proof automated calibration units (ACUs) are mounted on the top of each AD. Each ACU is equipped with an LED, a ⁶⁸Ge source, and a composite source of ²⁴¹Am–¹³C and ⁶⁰Co. Deployment of the source into the liquid scintillator, one at a time, is controlled remotely. With the ACUs, the AD can be fully submerged in water without a chimney for calibration. Therefore, Daya Bay does not experience backgrounds coming from external radioactivity or the Michel electrons from decays of stopped muon.

The inner wall of the stainless steel tank is painted black with a fluor-carbon paint. To reduce the stray light reflected from the PMT glass, cable, and other components, another light shield made of black, matte ABS is installed at the equator of the PMTs. This design has an unforeseen advantage of suppressing an instrumental background, the PMT flasher events, which appeared in many neutrino experiments using PMTs but become difficult to reject for relatively small detectors. The electronic components or connections on the base of the Hamamatsu PMT may occasionally discharge and produce a flash of light. The detected energy of these events ranges from sub-MeV to a hundred MeV in Daya Bay. Although only a small fraction of the PMTs spontaneously discharge infrequently, these flasher events significantly increase the accidental-coincidence background. With the black shield, the flasher events always appear as a characteristic PMT-hit pattern; thus they can be easily identified and rejected [18]. Without this unique PMT-hit pattern, we would have to either turn off the flashing PMTs, or bear a larger uncertainty in the selection efficiency and a larger accidental-coincidence background.

4. Signal and background

The reactor antineutrinos are detected via the inverse β -decay (IBD) reaction, $\bar{\nu}_e + p \rightarrow e^+ + n$, in the Gd-LS. The coincidence of the prompt scintillation from the e^+ and the delayed

neutron capture on Gd provides a distinctive signature. The positron carries almost all the energy of the antineutrino, thus the positron energy deposited in the liquid scintillator is highly correlated with the antineutrino energy. The neutron thermalizes before being captured on either a proton or a gadolinium nucleus with a mean capture time of $\sim 30 \mu\text{s}$ in Gd-LS or $\sim 200 \mu\text{s}$ in normal LS. When a neutron is captured on Gd, the process releases several gamma-rays with a total energy of $\sim 8 \text{ MeV}$, and is thus easily distinguished from the background coming from natural radioactivity. The capture on H suffers from a larger background but provides an independent measurement and can improve the precision of the θ_{13} measurement.

The ADs are calibrated with sources in the ACUs weekly, and with spallation products, IBDs, and natural radiation from materials inside the detectors. Two independent calibration algorithms are utilized. The energy scale is determined using the ^{60}Co or Am-C neutron source in the ACUs, or spallation neutrons. The uncertainty in the energy scale is determined by comparing more than 10 known references in the 8 ADs and by studying their stabilities over time. The uncertainty in the energy scale has reduced from 0.5% reported in the initial publications [16,17] to 0.2% in the latest [21]. The reduction comes from the improvements in the correction of position and time dependence.

Nonlinearity in the energy response of an AD originates from two dominant sources: particle-dependent nonlinear light yield of the scintillator and charge-dependent nonlinearity in the PMT readout electronics. Each effect is on the order of 10% at low energy. We have constructed a semi-empirical model that predicts the reconstructed energy for a particle assuming a specific energy deposited in the scintillator. The model contains four parameters: Birks' constant, the relative contribution to the total light yield from Cherenkov radiation, and the amplitude and scale of an exponential correction describing the non-linear electronics response. This exponential form of the electronics response is motivated by Monte Carlo (MC) and data; it has been confirmed with an independent FADC measurement. Besides the calibration references used in the energy scale studies, a broad set of calibration sources were deployed into the two ADs of EH1 using the ACUs and a manual calibration system [31] during the shutdown in the summer of 2012. The energy nonlinearity, i.e. the absolute energy scale, is determined to $< 1\%$ above 2 MeV.

To select reactor antineutrino events, the PMT flasher background is rejected first. The prompt and delayed signals are required to be 0.7–12 MeV and 6–12 MeV, respectively. The temporal separation between a pair of prompt and delayed signals should be within 1–200 μs . To reject cosmogenic background, the delayed signal is required to be 600 μs , 1000 μs , or 1 s later than a muon, depending on the deposited energy of the muon. Finally, no other signal should occur in within 200 μs before the prompt signal and after the delayed signal. Two independent algorithms are developed following these criteria with minor differences. The selected samples differ by less than 10%, mostly due to the different energy calibration used.

A detailed treatment of the absolute and relative efficiencies was reported in Refs. [16,18]. The uncertainties of the absolute efficiencies are correlated among the ADs and are thus negligible in oscillation analyses. The determination of all relative uncertainties is data-driven. The dominant ones come from the energy calibration and the neutron capture fraction on Gd, both at the 0.1% level. The total relative uncertainty is conservatively estimated to be 0.2%, uncorrelated among the ADs.

Five kinds of background are considered in Daya Bay. The accidental background is the largest one but contributes negligible to the total systematic uncertainty. The most serious background is the cosmogenic $^9\text{Li}/^8\text{He}$, which contributes an uncertainty of $\sim 0.2\%$. The remaining three kinds of background have an uncertainty of $\sim 0.01\%$.

The accidental background, from accidental correlation of two unrelated signals, is determined by measuring the rate of both prompt- and delayed-like signals, and then estimating the probability that two signals randomly satisfy the time coincidence for the IBD selection.

The ${}^9\text{Li}/{}^8\text{He}$ background comes from the β - n decay of ${}^9\text{Li}/{}^8\text{He}$ produced by muons in the ADs. The rate is evaluated from the distribution of the time since the last muon using the known lifetimes of these isotopes. A 50% systematic uncertainty is assigned to account for the extrapolation to zero deposited muon energy.

An energetic neutron entering an AD can form a fast-neutron background by recoiling off a proton before being captured. It is estimated by extrapolating the prompt energy spectrum into the IBD energy region, or by studying the muon-tagged fast-neutron sample.

The ${}^{13}\text{C}(\alpha, n){}^{16}\text{O}$ background was determined using MC after estimating the amount of ${}^{238}\text{U}$, ${}^{232}\text{Th}$, ${}^{227}\text{Ac}$, and ${}^{210}\text{Po}$ in the Gd-LS from their cascade decays, or by fitting their α -particle energy peaks in the data.

A neutron emitted from the Am-C neutron source in an ACU could generate a gamma-ray via inelastic scattering in the stainless steel vessel before subsequently being captured on Fe/Cr/Mn/Ni. An IBD is mimicked if both gamma-rays from the scattering and capture processes enter the scintillator. This correlated background is estimated using MC. The normalization is constrained by the measured rate of single delayed-like candidates from this source.

5. Oscillation analyses

Early results of Daya Bay were based on rate analysis when the statistics were low. The rate deficit at the far site was $\sim 6\%$ compared to the prediction based on a weighted combination of two near-site measurements. The value of $\sin^2 2\theta_{13}$ is determined with a χ^2 constructed with pull terms accounting for the correlation of the systematic errors,

$$\chi^2 = \sum_{d=1}^6 \frac{[M_d - T_d (1 + \varepsilon + \sum_r \omega_r^d \alpha_r + \varepsilon_d) + \eta_d]^2}{M_d + B_d} + \sum_r \frac{\alpha_r^2}{\sigma_r^2} + \sum_{d=1}^6 \left(\frac{\varepsilon_d^2}{\sigma_d^2} + \frac{\eta_d^2}{\sigma_B^2} \right), \quad (3)$$

where M_d are the measured number of IBD events of the d -th AD with its backgrounds subtracted, B_d is the corresponding background, T_d is the prediction from antineutrino flux, including MC corrections for energy responses and neutrino oscillations, ω_r^d is the fraction of IBD contribution of the r -th reactor to the d -th AD determined by the baselines and antineutrino fluxes. The uncorrelated reactor uncertainty is σ_r (0.8%). The parameter σ_d (0.2%) is the uncorrelated detection uncertainty. The parameter σ_B ($\sim 0.2\%$) is the quadratic sum of the background uncertainties, which are site-dependent. The corresponding pull parameters are $(\alpha_r, \varepsilon_d, \eta_d)$. The absolute normalization ε , which absorbs the detector- and reactor-related correlated uncertainties, is a free parameter determined from the fit to the data. While keeping ε free, the reactor antineutrino flux is determined by the near-site measurements. The model-dependent reactor flux prediction enters the fit only at secondary order.

With increased statistics, the latest Daya Bay analyses are based on rate and shape analysis. While rate deficit still dominates the θ_{13} sensitivity, the spectral information starts to contribute. To take advantage of the spectral information, an analysis with a similar χ^2 expression as defined in Eq. (3) but with energy bins and relevant uncertainties is used. Additional inputs to the fit include the background shape uncertainties and energy nonlinearity model described in Sec. 4. Besides improving the precision of the $\sin^2 2\theta_{13}$, the effective mass splitting Δm_{ee}^2 has been measured for the first time [20].

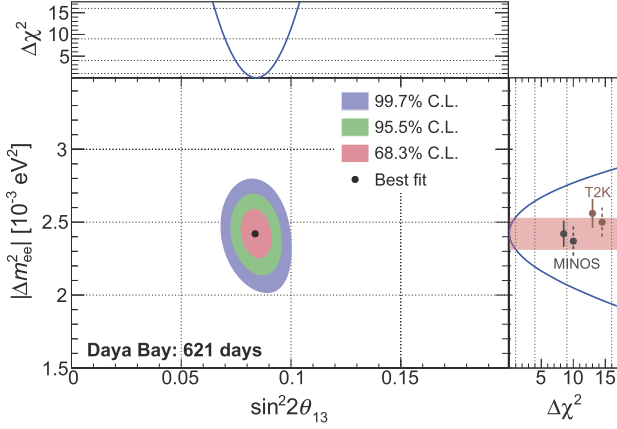


Fig. 3. Error contours corresponding to the 68.3%, 95.5% and 99.7% confidence levels in the $|\Delta m_{ee}^2|$ – $\sin^2 2\theta_{13}$ plane. The contours were obtained with a least-squares fit given in Eq. (4) using the measured $\bar{\nu}_e$ rates and energy spectra at the near and far sites. The adjoining panels show the dependence of $\Delta\chi^2$ on $\sin^2 2\theta_{13}$ (top) and $|\Delta m_{ee}^2|$ (right). Figure adapted from [21].

Another approach in extracting the oscillation parameters is to construct a χ^2 expression using a covariance matrix

$$\chi^2 = \sum_{i,j} (N_j^f - w_j \cdot N_j^n) (V^{-1})_{ij} (N_i^f - w_i \cdot N_i^n), \quad (4)$$

where N_i is the observed number of events after background subtraction in the i -th bin of reconstructed positron energy. The superscript $f(n)$ denotes a far (near) detector. The symbol V represents a covariance matrix that includes known systematic and statistical uncertainties. The quantity w_i is a weight that accounts for the differences between the near- and far-site measurements. In this method, the flux and spectrum of the antineutrinos at the reactor play a negligible role [21]. The results from the fit shown in the $\sin^2 2\theta_{13}$ – Δm_{ee}^2 plane are depicted in Fig. 3.

Daya Bay has also accumulated an IBD sample with neutron capture on hydrogen (nH) which has comparable statistics to that of neutron capture on gadolinium (nGd). Since the delayed signal of 2.2 MeV falls into the energy region totally dominated by natural radiation, the coincidence background is huge. By requiring the reconstructed distance between the positron and delayed-neutron vertices be < 50 cm, 98% of this background can be rejected while losing 25% of the signal. A spectral subtraction is further needed to remove the accidental backgrounds. An analysis using the 217-day data set yielded $\sin^2 2\theta_{13} = 0.080 \pm 0.018$. Since the IBD sample and the systematic uncertainties are largely independent from the nGd analysis, the nH analysis provides an independent measurement of θ_{13} . The correlation between the nH and nGd analyses is evaluated to be 0.05. When the nH and nGd analyses of this data set are combined, the $\sin^2 2\theta_{13}$ sensitivity is improved by 8% [19].

6. Reactor antineutrino spectrum and exotic searches

Although the oscillation analyses of Daya Bay have negligible dependence on the external prediction of the reactor antineutrino flux and spectrum, knowledge of these two quantities is a crucial factor for many reactor neutrino experiments. In the early studies, estimation of the flux and spectrum of the reactor antineutrinos relied on calculations or other indirect means, such as

the β spectrum measurements made on the major fissile isotopes after activation, based on the understanding of the complex fission processes in the reactor core. These methods have rather strong dependence on the theoretical models.

In the operating reactor cores, antineutrinos are emitted from four primary fuel isotopes: ^{235}U , ^{238}U , ^{239}Pu , and ^{241}Pu . Each fission releases about 200 MeV energy ((0.2–0.5)% uncertainty). Fission rates can be estimated from the thermal-power measurement (0.5% uncertainty) and simulation of the evolution of the fuel composition in the core (0.6% uncertainty with the constraint of the total thermal power) [33]. The most uncertain elements are the rate and spectrum of antineutrinos emitted from each fission of the four isotopes. By fitting the measured β spectrum of the ^{235}U , ^{239}Pu , and ^{241}Pu fuel [34–36] to a set of β decays, along with a theoretical calculation for ^{238}U , two models, the ILL–Vogel and the Huber–Mueller models, have been developed [37–39] with an uncertainty of (2–3)%.

Daya Bay has accumulated the world’s largest sample of reactor antineutrinos, at a rate of ~ 1 million per year. A direct measurement will provide the most precise and model-independent reactor antineutrino spectrum. Recently, Daya Bay has determined the absolute reactor antineutrino rate to be $\sigma_f = (5.92 \pm 0.14) \times 10^{-43} \text{ cm}^2 \text{ fission}^{-1}$, where the dominant uncertainty comes from the absolute efficiency of 2.1% [22]. This result is consistent with the past 19 short-baseline (< 100 m) measurements. However, comparing to the Huber–Mueller model, there is a $\sim 6\%$ deficit.

With the nonlinear-response model described in Sec. 4, Daya Bay has measured the prompt-energy spectrum with a precision ranging from 1.0% at 3.5 MeV to 6.7% at 7 MeV. Comparing to the calculations described above, approximate 10% more events is observed at ~ 5 MeV, leading to a discrepancy of about 4σ . Such a deviation shows the importance of model-independent measurement of the reactor antineutrino spectrum, particularly for the next-generation reactor experiments such as JUNO [40]. Furthermore, it points to the need of revisiting the model-dependent calculations. When the prompt-energy spectrum is unfolded, i.e. removing the detector response and oscillation effects, an antineutrino spectrum at the core shown in Fig. 4 is obtained.

Daya Bay will improve the measurement with higher statistics and better energy response model. Recently, a Flash Analog-to-Digital Converter (FADC) system has been installed for processing the signals of one AD, with the goal of pinning down the nonlinearity of the electronics. Another calibration and systematic-study campaign is being planned. We expect to measure the reactor antineutrino spectrum to 1% precision over a broad energy range, especially improving the precision in the very high- and very low-energy regions where the current models do not address.

The high-precision antineutrino spectrum is also ideal for searching for light sterile neutrinos. If light sterile neutrinos mix with the three active neutrinos, their presence could be detected by looking for the fast oscillatory behavior in the spectrum. Daya Bay has significantly extended the exclusion area with $10^{-3} \text{ eV}^2 \lesssim |\Delta m_{41}^2| \lesssim 0.1 \text{ eV}^2$ [23]. Further improvements with increasing statistics are expected.

Besides the sterile-neutrino studies, more exotic searches are in progress, for example, non-standard interaction, decoherence effect, mass-varying neutrino, Lorentz-violation, and CPT violation.

7. Summary and prospect

With an almost ideal experimental site and unique design, the Daya Bay experiment has excellent capability for carrying out high-precision measurements of reactor antineutrinos. We have

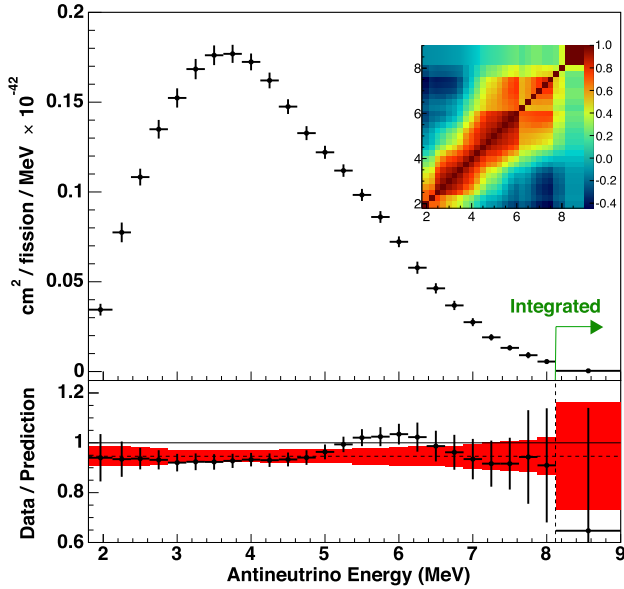


Fig. 4. Top panel: The extracted reactor antineutrino spectrum and its correlation matrix. Bottom panel: Ratio of the extracted reactor antineutrino spectrum to the Huber+Mueller prediction. Adapted from [22].

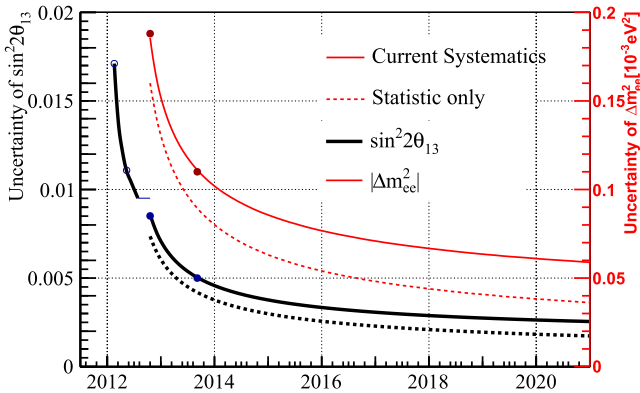


Fig. 5. Projected precision of $\sin^2 2\theta_{13}$ (black thick lines) and Δm_{ee}^2 (red thin lines) in Daya Bay, where the solid lines present the precision estimated with current systematics and the dashed lines show the statistical limit with zero systematic uncertainty. The points on the curves show the precision of published Daya Bay results. (For interpretation of the references to color in this figure legend, the reader is referred to the web version of this article.)

reviewed our design experience, which may help future reactor neutrino experiments. The measurements on θ_{13} and effective mass splitting are reviewed. The current precision on $\sin^2 2\theta_{13}$ and $|\Delta m_{ee}^2|$ are 6% and 4.5%, respectively. Our projected precisions of these two fundamental parameters are shown in Fig. 5. The Daya Bay experiment is expected to operate until 2020; by then, the precision is $\sim 3\%$ for both $\sin^2 2\theta_{13}$ and $|\Delta m_{ee}^2|$. Daya Bay has also obtained the most precise reactor antineutrino spectrum, which will be very valuable for designing the next-generation reactor neutrino experiments that depend on this input, such as JUNO.

Acknowledgements

We would like to thank Jie Zhao for preparing Fig. 5. J.C. is partially supported by the National Natural Science Foundation of China (11225525) and K.B.L. is partially supported by the U.S. Department of Energy, OHEP DE-AC02-05CH11231.

References

- [1] Y. Fukuda, et al., *Phys. Rev. Lett.* 81 (1998) 1562.
- [2] M.H. Ahn, et al., *Phys. Rev. Lett.* 90 (2003) 041801.
- [3] Q.R. Ahmad, et al., *Phys. Rev. Lett.* 89 (2002) 011301.
- [4] K. Eguchi, et al., *Phys. Rev. Lett.* 90 (2003) 021802.
- [5] M. Apollonio, et al., *Eur. Phys. J. C* 27 (2003) 331.
- [6] F. Boehm, et al., *Phys. Rev. D* 62 (2000) 072002.
- [7] L.A. Mikaelyan, V.V. Sinev, *Phys. At. Nucl.* 63 (2000) 1002.
- [8] K. Anderson, et al., White paper report on using nuclear reactors to search for a value of θ_{13} , arXiv:hep-ex/0402041.
- [9] X.H. Guo, et al., Daya Bay Collaboration, arXiv:hep-ex/0701029.
- [10] F. Ardellier, et al., Double Chooz Collaboration, arXiv:hep-ex/0606025.
- [11] S.B. Kim, RENO Collaboration, *AIP Conf. Proc.* 981 (2008) 205.
- [12] <http://dayabay.ihep.ac.cn/hk2003/>.
- [13] Workshop webpage, <http://dayabay.ihep.ac.cn/ihep2004/>.
- [14] The neutrino matrix, <http://www.aps.org/policy/reports/multidivisional/neutrino/index.cfm>.
- [15] <http://www.science.doe.gov/hep/NuSAG2ndRptFeb2006.pdf>.
- [16] F.P. An, et al., Daya Bay Collaboration, *Nucl. Instrum. Methods A* 685 (2012) 78.
- [17] F.P. An, et al., Daya Bay Collaboration, *Phys. Rev. Lett.* 108 (2012) 171803.
- [18] F.P. An, et al., Daya Bay Collaboration, *Chin. Phys. C* 37 (2013) 011001.
- [19] F.P. An, et al., Daya Bay Collaboration, *Phys. Rev. D* 90 (2014) 071101.
- [20] F.P. An, et al., Daya Bay Collaboration, *Phys. Rev. Lett.* 112 (2014) 061801.
- [21] F.P. An, et al., Daya Bay Collaboration, *Phys. Rev. Lett.* 115 (2015) 111802.
- [22] F.P. An, et al., Daya Bay Collaboration, *Phys. Rev. Lett.* 116 (2016) 061801.
- [23] F.P. An, et al., Daya Bay Collaboration, *Phys. Rev. Lett.* 113 (2014) 141802.
- [24] P. Huber, M. Lindner, T. Schwetz, W. Winter, *Nucl. Phys. B* 665 (2003) 487.
- [25] Y.X. Sun, et al., *HEPNP* 29 (2005) 543.
- [26] F.P. An, et al., Daya Bay Collaboration, *Nucl. Instrum. Methods A* 811 (2016) 133.
- [27] Y.Y. Ding, et al., *J. Rare Earths* 25 (2007) 310.
- [28] Y.Y. Ding, et al., *Nucl. Instrum. Methods A* 584 (2008) 238.
- [29] M. Yeh, et al., *Nucl. Instrum. Methods A* 578 (2007) 329.
- [30] W. Beriguete, et al., *Nucl. Instrum. Methods A* 763 (2014) 82.
- [31] H.X. Huang, et al., *J. Instrum.* 8 (2013) P09013.
- [32] F.P. An, et al., Daya Bay Collaboration, *Nucl. Instrum. Methods A* 773 (2015) 8.
- [33] J. Cao, *Nucl. Phys. B, Proc. Suppl.* 229–232 (2012) 205.
- [34] W.G.K. Schreckenbach, G. Colvin, F. von Feilitzsch, *Phys. Lett. B* 160 (1985) 325.
- [35] A.F. von Feilitzsch, K. Schreckenbach, *Phys. Lett. B* 118 (1982) 162.
- [36] A.A. Hahn, et al., *Phys. Lett. B* 218 (1989) 365.
- [37] P. Vogel, G.K. Schenter, F.M. Mann, R.E. Schenter, *Phys. Rev. C* 24 (1981) 1543.
- [38] T. Mueller, et al., *Phys. Rev. C* 83 (2011) 054615.
- [39] P. Huber, *Phys. Rev. C* 84 (2011) 024617;
P. Huber, *Phys. Rev. C* 85 (2012) 029901 (Erratum).
- [40] F.P. An, et al., *J. Phys. G, Nucl. Part. Phys.* 43 (2016) 030401.